Interaction of half-quantized vortices in two-component Bose-Einstein condensates

Minoru Eto,[1,*] Kenichi Kasamatsu,[2] Muneto Nitta,[3] Hiromitsu Takeuchi,[4] and Makoto Tsubota[5]

[1]*Department of Physics, Yamagata University, Yamagata 990-8560, Japan*

[2]*Department of Physics, Kinki University, Higashi-Osaka, 577-8502, Japan*

[3]*Department of Physics, and Research and Education Center for Natural Sciences, Keio University, Hiyoshi 4-1-1, Yokohama, Kanagawa 223-8521, Japan*

[4]*Graduate School of Integrated Arts and Science, Hiroshima University, Kagamiyama, 1-7-1, Higashi Hiroshima, 739-8521, Japan*

[5]*Department of Physics, Osaka City University, Sumiyoshi-Ku, Osaka 558-8585, Japan*

(Received 31 March 2011; published 3 June 2011)

We study the asymptotic interaction between two half-quantized vortices in two-component Bose-Einstein condensates. When two vortices in different components are placed at distance $2R$, the leading order of the force between them is found to be $(\ln R/\xi - 1/2)/R^3$, in contrast to $1/R$ between vortices placed in the same component. We derive it analytically using the Abrikosov ansatz and the profile functions of the vortices, confirmed numerically with the Gross-Pitaevskii model. We also find that the short-range cutoff of the intervortex potential linearly depends on the healing length.

DOI: 10.1103/PhysRevA.83.063603 PACS number(s): 03.75.Lm, 03.75.Mn, 67.85.Fg

I. INTRODUCTION

Multicomponent condensations appear in many systems in condensed matter physics and quantum chromodynamics (QCD), from multicomponent or spinor Bose-Einstein condensates (BECs), superfluid ^{3}He, and multigap superconductors to chiral phase transition or color superconductors in QCD at high temperature and/or high density. Especially, multicomponent and spinor BECs admit a rich variety of topological excitations: domain walls [1], Abelian [2] and non-Abelian [3] vortices, monopoles [4], 2D Skyrmions [5], 3D Skyrmions [6,7], vortons [8], knots [9], and D-brane solitons [10]. See Refs. [2,11,12] for reviews. Among these topological excitations, quantized vortices in multicomponent BECs are the most important subject, because they are closely related to the problems not only in other condensed matter systems such as superconductors, superfluids, magnetism, and liquid crystal, but also in electroweak theory [13], QCD, and grand unified theories in high-energy physics, neutron stars, and cosmic strings in cosmology [14,15].

Interactions between quantized vortices are important information to determine the equilibrium configuration and dynamics of many vortices. It is known that, in a single-component BEC, the asymptotic interaction energy per unit length of two parallel vortex lines separated by a distance R is proportional to $\ln(L/R)$, where L is the size of the system [16]. Thus, the intervortex force has $1/R$ dependence. Vortices in a BEC resemble with global vortices in relativistic field theories [17–20]. A relation between them was studied in Ref. [20], where it was suggested that spinning global vortices on a Lorentz violating background behave as superfluid vortices. Global vortices are regarded as global cosmic strings or axion strings in cosmology and the intervortex force between two global vortices was shown to be $1/R$ [18], coinciding with the one in vortices in a scalar BEC, scalar superfluid, and the XY model. Global vortices also appear in QCD—in chiral-phase transition of QCD at high temperature or high density [21,22] or color superconductor of extremely high density QCD [23,24]. Intervortex force at large distance R was derived analytically at the leading order as $1/R$ for color superconductor [24] and $\cos\alpha/R$ with a relative orientation α of two vortices in the internal space for chiral-phase transition [22]; see Ref. [25] for a review.

However, the analytic formula of the vortex-vortex interactions in multicomponent BECs are still missing. Two-component BECs are the simplest example of the multicomponent condensates and have also attracted much interest to study the novel phenomena not found in a single component BEC. Recent experiments provide a good ground of study on the vortex-vortex interaction in two-component BECs by tuning s-wave scattering length via a Feshbach resonance [26–28]. The minimally quantized vortex in two-component BECs has the winding number one half of a singly quantized vortex in scalar BECs, and thus is often called a half-quantized vortex. Its mass circulation is fractionally quantized when mass densities of two condensates are different. Such a quantized vortex in two-component BECs has a composite structure, where a vortex core in one component is filled by the density of the other component. This vortex structure was created experimentally through coherent interconversion between two components [29]. Interactions between the vortices in the different components are nontrivial because the two components interact only through the density, so that the vortex winding around one component does not directly experience the circulation of the other vortex winding around the other component. This fact results in an indirect interaction, where the filling component of each vortex core is affected by the circulation created by the vortex in the *same* component, dragging the vortex in which it is filled. Although the interactive dynamics of two vortices in two-component BECs was studied numerically by Öhberg and Santos [30], the analytical form of the interaction force was not discussed.

In this paper, we consider the asymptotic interaction between two vortices in two-component BECs. We consider the vortex-vortex interaction for two cases: (i) two vortices are placed in the different components and (ii) those in the same component. For the case (i), the leading order of the intervortex force between them at distance $2R$ is found to be

[*]On leave from Mathematical Physics Lab., RIKEN Nishina center.

$(\ln R/\xi - 1/2)/R^3$ with the short-range cutoff ξ, in contrast to the one $1/R$ for the case (ii) and vortices in a single-component BEC. We derive it analytically using the Abrikosov ansatz and the asymptotic profile functions of the vortices. We then confirm it numerically. We also find that the short-range cutoff ξ of the intervortex potential linearly depends on the healing length.

This paper is organized as follows. Section II is devoted to deriving the analytic form of the asymptotic intervortex force. In Sec. III, we confirm the analytic results obtained in Sec. II by numerical calculations of the Gross-Pitaevskii equation. Summary and discussions are in Sec. IV. In the Appendix, we describe some details of the calculation of integrals in Sec. II C.

II. STATIC INTERVORTEX FORCES

A. The model

We start with an energy functional for two-component BEC system,

$$E(\Psi_1,\Psi_2) = K(\Psi_1,\Psi_2) + V(\Psi_1,\Psi_2), \tag{1}$$

$$K = \int d^3x \sum_{i=1,2}\left(-\frac{\hbar^2}{2m_i}\Psi_i^*\nabla^2\Psi_i\right), \tag{2}$$

$$V = \int d^3x \left[\sum_{i=1,2}\frac{g_i}{2}|\Psi_i|^4 + g_{12}|\Psi_1|^2|\Psi_2|^2\right], \tag{3}$$

where Ψ_i is a condensate wave function of the i-th component ($i = 1,2$) with mass m_i. The coupling constants g_1, g_2, and g_{12} stand for the atom-atom interactions; the Ψ_1 and Ψ_2 components repel or attract for $g_{12} > 0$ or $g_{12} < 0$, respectively. The coupled Gross-Pitaevskii (GP) equations are obtained by the variational principle $i\hbar\partial_t\Psi_i = \delta E/\delta\Psi_i^*$ as

$$i\hbar\partial_t\Psi_1 = \left(-\frac{\hbar^2\nabla^2}{2m_1} + g_1|\Psi_1|^2 + g_{12}|\Psi_2|^2\right)\Psi_1, \tag{4}$$

$$i\hbar\partial_t\Psi_2 = \left(-\frac{\hbar^2\nabla^2}{2m_2} + g_2|\Psi_2|^2 + g_{12}|\Psi_1|^2\right)\Psi_2. \tag{5}$$

The stationary coupled GP equation is given by considering a time-dependence $\Psi_i(\mathbf{x},t) = e^{-i\mu_i t/\hbar}\Psi_i(\mathbf{x})$ with the chemical potential μ_i:

$$\left[-\frac{\hbar^2\nabla^2}{2m_1} - \mu_1 + g_1|\Psi_1(\mathbf{x})|^2 + g_{12}|\Psi_2(\mathbf{x})|^2\right]\Psi_1(\mathbf{x}) = 0, \tag{6}$$

$$\left[-\frac{\hbar^2\nabla^2}{2m_2} - \mu_2 + g_2|\Psi_2(\mathbf{x})|^2 + g_{12}|\Psi_1(\mathbf{x})|^2\right]\Psi_2(\mathbf{x}) = 0. \tag{7}$$

The potential energy V with the quadratic terms $-\mu_1|\Psi_1|^2 - \mu_2|\Psi_2|^2$ induced by the chemical potential is a quadratic function of $X \equiv |\Psi_1|^2 \geqslant 0$ and $Y \equiv |\Psi_2|^2 \geqslant 0$:

$$V(X,Y) = \frac{g_1}{2}X^2 + \frac{g_2}{2}Y^2 + g_{12}XY - \mu_1 X - \mu_2 Y. \tag{8}$$

Let g_1, g_2 be positive, then the potential V has a minimum when

$$\Delta \equiv V_{XX}V_{YY} - V_{XY}^2 = g_1g_2 - g_{12}^2 > 0,$$
$$\mu_1 g_2 - \mu_2 g_{12} \geqslant 0, \quad \mu_2 g_1 - \mu_1 g_{12} \geqslant 0. \tag{9}$$

The amplitudes of the ground state are then given by

$$|\Psi_1| = \sqrt{\frac{\mu_1 g_2 - \mu_2 g_{12}}{g_1g_2 - g_{12}^2}} \equiv v_1,$$
$$|\Psi_2| = \sqrt{\frac{\mu_2 g_1 - \mu_1 g_{12}}{g_1g_2 - g_{12}^2}} \equiv v_2. \tag{10}$$

In the following, we consider the situation in which the above inequalities are satisfied. Since there are two condensates, two $U(1)$ symmetries are spontaneously broken. Accordingly, the order parameter space is

$$T^2 \simeq U(1)_1 \times U(1)_2 \simeq \frac{U(1)_{\text{mass}} \times U(1)_{\text{spin}}}{\mathbb{Z}_2}. \tag{11}$$

Here, each $U(1)_i$ ($i = 1,2$) corresponds to the phase rotation of Ψ_1 or Ψ_2, while $U(1)_{\text{mass}}$ and $U(1)_{\text{spin}}$ correspond to the overall and relative phase rotations, defined by

$$U(1)_{\text{mass}}: \quad \Psi_1 \to \Psi_1 e^{i\alpha}, \quad \Psi_2 \to \Psi_2 e^{i\alpha},$$
$$U(1)_{\text{spin}}: \quad \Psi_1 \to \Psi_1 e^{i\beta}, \quad \Psi_2 \to \Psi_2 e^{-i\beta}, \tag{12}$$

whose currents are mass and pseudo-spin currents, respectively. Both the condensates Ψ_1, Ψ_2 are unchanged under the $\mathbb{Z}_2$ action ($\alpha = \beta = \pi$) inside $U(1)_{\text{mass}} \times U(1)_{\text{spin}}$ in Eq. (12), and therefore, this $\mathbb{Z}_2$ has to be removed as the denominator of Eq. (11).

In what follows, we call the phase cycles for Ψ_1 and Ψ_2 the (1,0) and (0,1) cycles, respectively.

B. Vortex configuration

Since the first homotopy group of order parameter space is

$$\pi_1(T^2) = \mathbb{Z} \oplus \mathbb{Z}, \tag{13}$$

it allows two kinds of winding numbers. We refer a vortex winding around (1,0)[(0,1)] cycle once as a (1,0) vortex [(0,1) vortex], which is the most fundamental vortex. When one travels around a (1,0)[(0,1)] vortex, the phase of $\Psi_1(\Psi_2)$ rotates by 2π with the phase of the other component kept constant. On the other hand, in terms of $U(1)_{\text{mass}}$ and $U(1)_{\text{spin}}$ in Eq. (12), $U(1)_{\text{mass}}$ is rotated by π and $U(1)_{\text{spin}}$ is rotated by $+\pi$ $(-\pi)$ with circling around a (1,0)[(0,1)] vortex. Since they have a half winding of $U(1)_{\text{mass}}$, they are often called *half-quantized* vortices.

Vortices winding around both components by 2π are denoted by (1,1) and have unit winding in $U(1)_{\text{mass}}$. They are called integer vortices, if the core is not separated into (1,0) and (0,1) vortices. More generally, we refer to a configuration that winds (1,0) cycle m times and (0,1) cycle n times as an (m,n) vortex, whose wave function is denoted as $\Psi_i^{(m,n)}$ for the i-th component.

The vortex configuration can be obtained by solving Eqs. (6) and (7). Let us make an ansatz for an axially symmetric (1,0)-vortex configuration:

$$\Psi_1^{(1,0)} = v_1\, e^{i\theta} f_{(1,0)}(r), \quad \Psi_2^{(1,0)} = v_2\, h_{(1,0)}(r), \tag{14}$$

where r and θ are the polar coordinates. The profile functions $f_{(1,0)}$ and $h_{(1,0)}$ are determined by substituting (14) into (6) and (7), as

$$-\frac{\hbar^2}{2m_1}\left(f''_{(1,0)}+\frac{f'_{(1,0)}}{r}-\frac{f_{(1,0)}}{r^2}\right)+\frac{\mu_1 g_1 g_2\left(f^2_{(1,0)}-1\right)-\mu_1 g_{12}^2\left(h^2_{(1,0)}-1\right)-\mu_2 g_1 g_{12}\left(f^2_{(1,0)}-h^2_{(1,0)}\right)}{g_1 g_2-g_{12}^2}f_{(1,0)}=0, \tag{15}$$

$$-\frac{\hbar^2}{2m_2}\left(h''_{(1,0)}+\frac{h'_{(1,0)}}{r}\right)+\frac{\mu_2 g_1 g_2\left(h^2_{(1,0)}-1\right)-\mu_2 g_{12}^2\left(f^2_{(1,0)}-1\right)-\mu_1 g_2 g_{12}\left(h^2_{(1,0)}-f^2_{(1,0)}\right)}{g_1 g_2-g_{12}^2}h_{(1,0)}=0, \tag{16}$$

with the prime denoting a differentiation with respect to r. We solve these equations with the boundary conditions

$$(f_{(1,0)},h_{(1,0)})\to(1,1) \qquad \text{as} \quad r\to\infty, \tag{17}$$

$$(f_{(1,0)},h'_{(1,0)})\to(0,0) \qquad \text{as} \quad r\to 0. \tag{18}$$

From these equations, asymptotic behaviors of the profile functions $f_{(1,0)}$ and $h_{(1,0)}$ at large distance can be obtained as

$$f_{(1,0)}(r)=1-\frac{1}{m_1\eta_1^+ r^2}+O(r^{-4}), \tag{19}$$

$$h_{(1,0)}(r)=1+\frac{1}{m_1\eta_1^- r^2}+O(r^{-4}), \tag{20}$$

where we have introduced the effective mass parameters

$$\eta_1^+\equiv\frac{4(\mu_1 g_2-\mu_2 g_{12})}{g_2\hbar^2}, \quad \eta_1^-\equiv\frac{4(\mu_2 g_1-\mu_1 g_{12})}{g_{12}\hbar^2}. \tag{21}$$

The stability condition Eq. (9) of the ground state ensures that $\eta_1^+>0$, while η_1^- changes its sign with g_{12}.

Similarly, we make an ansatz for the (0,1) vortex:

$$\Psi_1^{(0,1)}=v_1 h_{(0,1)}(r), \quad \Psi_2^{(0,1)}=v_2 e^{i\theta}f_{(0,1)}(r). \tag{22}$$

The equations for $f_{(0,1)},h_{(0,1)}$ can be obtained by just replacing the indices as $1\leftrightarrow 2$ and $(1,0)\leftrightarrow(0,1)$ in Eqs. (15) and (16). Then the asymptotic behaviors are

$$f_{(0,1)}(r)=1-\frac{1}{m_2\eta_2^+ r^2}+O(r^{-4}), \tag{23}$$

$$h_{(0,1)}(r)=1+\frac{1}{m_2\eta_2^- r^2}+O(r^{-4}), \tag{24}$$

with

$$\eta_2^+\equiv\frac{4(\mu_2 g_1-\mu_1 g_{12})}{g_1\hbar^2}, \quad \eta_2^-\equiv\frac{4(\mu_1 g_2-\mu_2 g_{12})}{g_{12}\hbar^2}. \tag{25}$$

Again, η_2^+ is always positive while sign of η_2^- depends on g_{12}.

As vortices in a scalar BEC, the tension (energy per unit length) of (1,0) and (0,1) vortices logarithmically diverges as

$$T_{(1,0)}\simeq\frac{\pi\hbar^2 v_1^2}{m_1}\ln\frac{L}{\xi}, \qquad T_{(0,1)}\simeq\frac{\pi\hbar^2 v_2^2}{m_2}\ln\frac{L}{\xi}, \tag{26}$$

respectively, with L and ξ being a long and short distance cutoff, respectively. This divergent behavior comes from the kinetic term in the GP energy functional Eq. (3).

Some numerical solutions of the single-vortex configurations are shown in Fig. 1. A universal feature of configuration is that $h_{(1,0)}$ (the profile function of unwinding field) at the vortex center is concave for $g_{12}<0$ and convex for the $g_{12}>0$ [31]. This can be understood from the atom-atom interaction g_{12}; in the presence of the vortex profile for Ψ_1 as a background, Ψ_2 feels the potential $g_{12}|\Psi_1|^2$ and it tends to be trapped in the vortex center for the repulsive interaction $g_{12}>0$ and to be exclusive from the vortex center for the attractive interaction $g_{12}<0$.

C. Intervortex forces

It is expected that the interactions between (1,0) and (0,1) vortices are determined by the coupling g_{12}-term. When g_{12} is zero, they are decoupled in Eqs. (4) and (5), so (1,0) and (0,1) vortices do not interact. Here, we calculate the asymptotic interactions between well-separated (1,0) and (0,1) vortices using their asymptotic profile functions obtained in the last subsection. Let us place the (1,0) and (0,1) vortices at $(x,y)=(R,0)$ and $(x,y)=(-R,0)$, respectively, as in Fig. 2. We use the polar coordinates (r,θ) with the origin $(x,y)=(0,0)$. We further express $[r_{(1,0)},\theta_{(1,0)}]$ and $[r_{(0,1)},\theta_{(0,1)}]$ as the polar coordinates with the origins at the (1,0) and (0,1) vortex centers $(R,0)$ and $(-R,0)$, respectively. Then the following relations hold among three polar coordinates:

$$\begin{aligned} r_i^2&=(r\cos\theta\mp R)^2+r^2\sin^2\theta,\\ \tan\theta_i&=\frac{r\sin\theta}{r\cos\theta\mp R}, \end{aligned} \tag{27}$$

with $i=(1,0),(0,1)$, the minus sign for $i=(1,0)$, and the plus sign for $i=(0,1)$. With these coordinates, the (1,0)- and (0,1)-vortex configurations $(\Psi_1^{(1,0)},\Psi_2^{(1,0)})$ and $(\Psi_1^{(0,1)},\Psi_2^{(0,1)})$ can be expressed as

$$\begin{aligned} \Psi_1^{(1,0)}&=v_1 e^{i\theta_{(1,0)}}f_{(1,0)}[r_{(1,0)}],\\ \Psi_2^{(1,0)}&=v_2 h_{(1,0)}[r_{(1,0)}], \end{aligned} \tag{28}$$

$$\begin{aligned} \Psi_1^{(0,1)}&=v_1 h_{(0,1)}[r_{(0,1)}],\\ \Psi_2^{(0,1)}&=v_2 e^{i\theta_{(0,1)}}f_{(0,1)}[r_{(0,1)}]. \end{aligned} \tag{29}$$

Let us now calculate the interaction between (1,0) vortex and (0,1) vortex. We first make the standard Abrikosov ansatz,

$$\begin{aligned} \Psi_1^{(1,1)}(r,\theta)&=v_1^{-1}\Psi_1^{(1,0)}\Psi_1^{(0,1)}\\ &\simeq v_1\left[1-\frac{1}{m_1\eta_1^+ r_{(1,0)}^2}+\frac{1}{m_2\eta_2^- r_{(0,1)}^2}\right]\\ &\quad\times e^{i\theta_{(1,0)}}+O(r^{-4}), \end{aligned} \tag{30}$$

$$\begin{aligned} \Psi_2^{(1,1)}(r,\theta)&=v_2^{-1}\Psi_2^{(1,0)}\Psi_2^{(0,1)}\\ &\simeq v_2\left[1-\frac{1}{m_2\eta_2^+ r_{(0,1)}^2}+\frac{1}{m_1\eta_1^- r_{(1,0)}^2}\right]\\ &\quad\times e^{i\theta_{(0,1)}}+O(r^{-4}), \end{aligned} \tag{31}$$

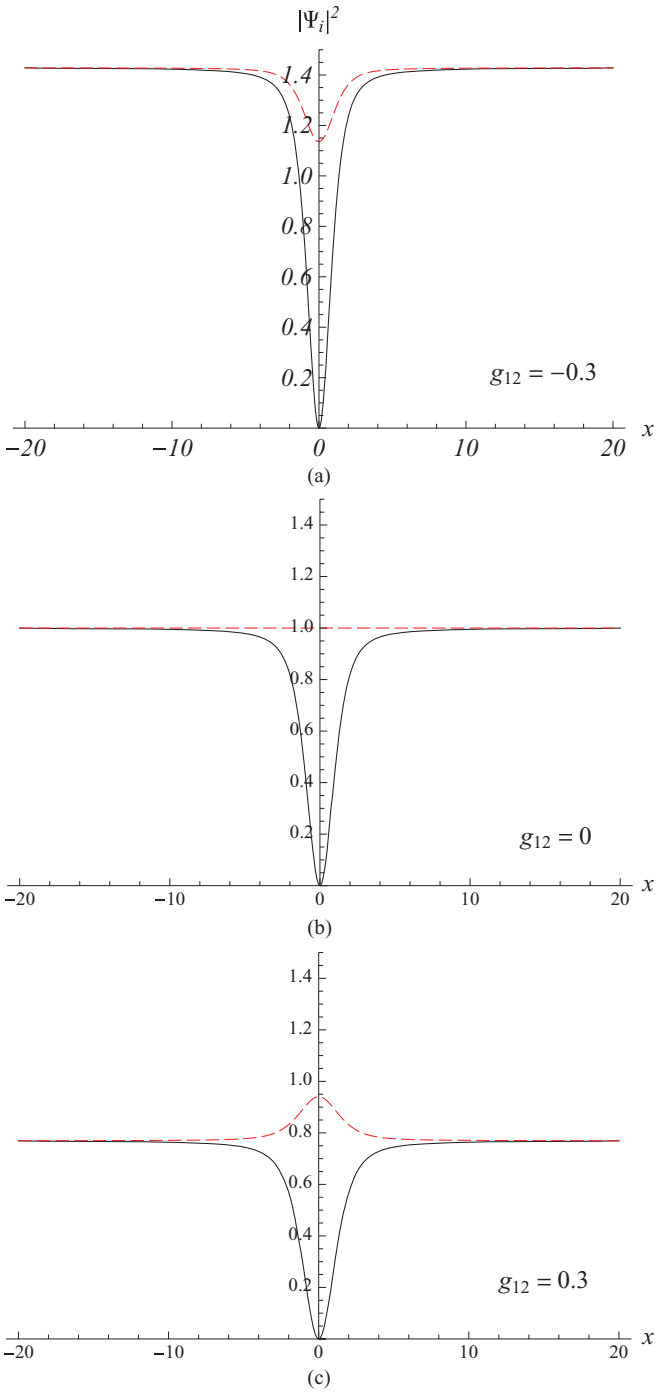

FIG. 1. (Color online) Single vortex configurations [$|\Psi_1|^2$ (solid line) and $|\Psi_2|^2$ (broken line)] on a cross section. The field Ψ_1 winds once so that $|\Psi_1|$ goes to zero at the vortex center while Ψ_2 does not touch zero anywhere, but it can have nonzero amplitude at the vortex center. The parameters are $(\hbar, g_1, g_2, \mu_1, \mu_2, m_1, m_2) = (1,1,1,1,1,1,1)$ and (a) $g_{12} = -0.3$, (b) $g_{12} = 0$, and (c) $g_{12} = 0.3$.

for the total configuration. Then the interaction potential is obtained by subtracting two individual vortex energies from the total energy as

$$U_{(1,1)} = \int d^2x \, (\delta K + \delta V), \tag{32}$$

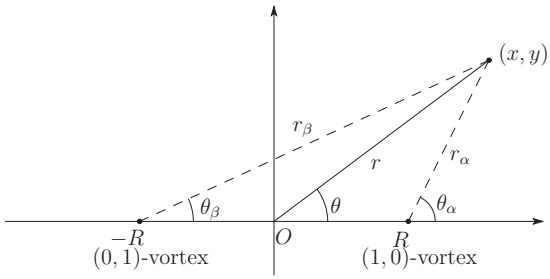

FIG. 2. Configuration of (1,0) vortex and (0,1) vortex.

where it has two contributions: one from the kinetic energy $\delta K = K(\Psi_1^{(1,1)}, \Psi_2^{(1,1)}) - K(\Psi_1^{(1,0)}, \Psi_2^{(1,0)}) - K(\Psi_1^{(0,1)}, \Psi_2^{(0,1)})$ and the other from the potential energy $\delta V = V(\Psi_1^{(1,1)}, \Psi_2^{(1,1)}) - V(\Psi_1^{(1,0)}, \Psi_2^{(1,0)}) - V(\Psi_1^{(0,1)}, \Psi_2^{(0,1)}) + V(v_1, v_2)$.

By using the asymptotic properties given in Eqs. (19), (20), (23), (24), (30), and (31), we find

$$\begin{aligned} \delta K &= \frac{v_1^2\hbar^2}{m_1 m_2 \eta_2^- r_{(0,1)}^2}[\nabla\theta_{(1,0)}]^2 \\ &\quad + \frac{v_2^2\hbar^2}{m_1 m_2 \eta_1^- r_{(1,0)}^2}[\nabla\theta_{(0,1)}]^2 + O(r^{-6}) \\ &= \frac{g_{12}\hbar^4}{2m_1 m_2 (g_1 g_2 - g_{12}^2) r_{(1,0)}^2 r_{(0,1)}^2} + O(r^{-6}), \end{aligned} \tag{33}$$

where we have used $[\nabla\theta_{(1,0)}]^2 = r_{(1,0)}^{-2}$, $[\nabla\theta_{(0,1)}]^2 = r_{(0,1)}^{-2}$ and have taken terms up to $O(r^{-4})$. It is important to see that the leading terms of the order $O(r^{-2})$ have been canceled out in the subtraction. Therefore, the dominant contribution to the interaction potential is of the order $O(r^{-4})$. Similarly, we find the terms of the order $O(r^{-4})$ in the potential energy

$$\delta V = -\frac{g_{12}\hbar^4}{4m_1 m_2 (g_1 g_2 - g_{12}^2) r_{(1,0)}^2 r_{(0,1)}^2} + O(r^{-6}). \tag{34}$$

Plugging these into Eq. (32), we get

$$\begin{aligned} U_{(1,1)}(R) &= \frac{g_{12}\hbar^4}{4m_1 m_2 (g_1 g_2 - g_{12}^2)} \int d^2x \, \frac{1}{r_{(1,0)}^2 r_{(0,1)}^2} \\ &\simeq \frac{g_{12}\hbar^4 \pi}{4m_1 m_2 (g_1 g_2 - g_{12}^2)} \frac{\ln \frac{R}{\xi}}{R^2}, \end{aligned} \tag{35}$$

where ξ stands for a short distance cut-off, and we have used $R \gg \xi$. The detailed calculation of Eq. (35) is described in the Appendix. Here, the terms independent of R have been ignored. The factor $1/R^2$ is a striking feature that is absent in the scalar BEC or scalar superfluids. Note that the chemical potentials μ_1 and μ_2 do not appear in the final result (35). The asymptotic force between the two vortices is obtained by differentiating the potential by their distance $2R$, as $F_{(1,1)}(R) = -\frac{dU_{(1,1)}}{2dR}$,

$$F_{(1,1)}(R) = \frac{\pi\hbar^4 g_{12}}{4m_1 m_2 (g_1 g_2 - g_{12}^2)} \frac{1}{R^3} \left(\ln \frac{R}{\xi} - \frac{1}{2} \right). \tag{36}$$

We have found that the interaction is attractive for $g_{12} < 0$, repulsive for $g_{12} > 0$, and vanishes for $g_{12} = 0$.

Note that the asymptotic interaction is independent of the sign of the vortex winding number $e^{\pm i\theta}$, because the interaction between the two condensates is mediated only through their amplitudes as $g_{12}|\Psi_1|^2|\Psi_2|^2$. In fact, the interaction potential $U_{(1,-1)}$ between (1,0) and (0, − 1) vortices are exactly the same as $U_{(1,1)}$. It is easy to verify that the following relation holds

$$U_{(1,1)} = U_{(1,-1)} = U_{(-1,1)} = U_{(-1,-1)}. \tag{37}$$

This is because $\theta_{(1,0)}$ and $\theta_{(0,1)}$ are decoupled in the Abrikosov ansatz in Eqs. (30) and (31).

The potential (35) should be compared with the potential $U_{(1\pm1,0)}$ between (1,0) and (±1,0) vortices. To see it, we make the ordinary Abrikosov ansatz

$$\Psi_1^{(1\pm1,0)} \simeq v_1 e^{i(\theta_{(1,0)}\pm\theta_{(0,1)})}, \qquad \Psi_2^{(1\pm1,0)} \simeq v_2. \tag{38}$$

Note here that we have taken terms of the order unity. A leading order contribution to the interaction comes from the kinetic term of Ψ_1, which is of order $O(r^{-2})$. On the other hand, the kinetic energy of Ψ_2 and the potential energy contributions start from the order $O(r^{-4})$, so we omit them. The interaction potential is then given by

$$\begin{aligned} U_{(1\pm1,0)} &= \pm\frac{v_1^2\hbar^2}{m_1}\int d^2x\ \vec{\nabla}\theta_{(1,0)}\cdot\vec{\nabla}\theta_{(0,1)} \\ &= \pm\frac{(\mu_1 g_2 - \mu_2 g_{12})\hbar^2\pi}{(g_1 g_2 - g_{12}^2)m_1}\ln\frac{R^2+L^2}{4R^2}, \end{aligned} \tag{39}$$

where L is an infrared cut-off parameter; see the Appendix for details. Unlike the case of the leading term in the potential (35) between (1,0) and (0,1) vortices, the potential $U_{(1\pm1,0)}$ depends on the chemical potential. We also note that it depends on the infrared cutoff L but not on the ultraviolet cutoff ξ.

The intervortex force $F_{(1\pm1,0)} = -\frac{dU_{(1\pm1,0)}}{2dR}$ is then

$$\begin{aligned} F_{(1\pm1,0)} &= \pm\frac{(\mu_1 g_2 - \mu_2 g_{12})\hbar^2\pi}{(g_1 g_2 - g_{12}^2)m_1}\left(\frac{1}{R} - \frac{R}{R^2+L^2}\right) \\ &\to \pm\frac{(\mu_1 g_2 - \mu_2 g_{12})\hbar^2\pi}{(g_1 g_2 - g_{12}^2)m_1}\frac{1}{R}, \end{aligned} \tag{40}$$

where $\to$ denotes the large volume limit $L\to\infty$. This $1/R$ force is well known for vortices in the scalar BEC, scalar superfluids, and the XY model, and global vortices in relativistic field theories [16,18]. The correction term for finite volume L can be found in the second term in the brace in the first line. This term might not be so familiar but has been obtained previously in [22] for global non-Abelian vortices in QCD.

In the same way, the interaction potential between (0,1) and (0, ± 1) vortices are given by

$$U_{(0,1\pm1)}(R) = \pm\frac{(\mu_2 g_1 - \mu_1 g_{12})\hbar^2\pi}{(g_1 g_2 - g_{12}^2)m_2}\ln\frac{R^2+L^2}{4R^2}. \tag{41}$$

III. NUMERICAL ANALYSIS

Let us numerically verify the interaction potential analytically obtained in Eq. (35). For simplicity, we consider a special case $m_1 = m_2 = m$, $g_1 = g_2 = g$, and $\mu_1 = \mu_2 = \mu$. Then the asymptotic behaviors of the profile functions in Eqs. (19) and (20) are rewritten as follows,

$$f_i + h_i = 2 - \frac{1}{m_+^2 r^2} + O(r^{-4}), \tag{42}$$

$$f_i - h_i = -\frac{1}{m_-^2 r^2} + O(r^{-4}), \tag{43}$$

for $i = (1,0)$ and $(0,1)$, where the mass parameters m_+ and m_- are defined by

$$m_+^2 \equiv \frac{4m\mu}{\hbar^2}, \quad m_-^2 \equiv \frac{4m\mu}{\hbar^2}\frac{g-g_{12}}{g+g_{12}}. \tag{44}$$

The inverse numbers of m_+ and m_- give the healing lengths associated with the mass component $f_i + h_i$ and the spin component $f_i - h_i$, respectively. The intervortex potential Eq. (35) is then expressed as

$$U_{(1,1)}(R) = \frac{\pi}{2}v^2\frac{m_+^2 - m_-^2}{m_+^2 m_-^2}\frac{1}{R^2}\ln\frac{R}{\xi}, \tag{45}$$

where $v^2 = \hbar^2\mu/m(g+g_{12})$ is defined in Eq. (10).

To obtain the intervortex potential numerically, we use a sort of the imaginary time propagation of the GP equation as

$$\begin{aligned} &\left[-\frac{\hbar^2}{2m}\nabla^2 - \mu + g|\Psi_1(\mathbf{x})|^2 + g_{12}|\Psi_2(\mathbf{x})|^2\right]\Psi_1(\mathbf{x},\tau) \\ &\quad = -D_1(\mathbf{x})\partial_\tau\Psi_1(\mathbf{x},\tau), \end{aligned} \tag{46}$$

$$\begin{aligned} &\left[-\frac{\hbar^2}{2m}\nabla^2 - \mu + g|\Psi_2(\mathbf{x})|^2 + g_{12}|\Psi_1(\mathbf{x})|^2\right]\Psi_2(\mathbf{x},\tau) \\ &\quad = -D_2(\mathbf{x})\partial_\tau\Psi_2(\mathbf{x},\tau), \end{aligned} \tag{47}$$

where τ is the imaginary time and D_1 and D_2 are positive coefficients. While D_i is set to be a constant in the usual imaginary time propagation, we consider the coefficient $D_i = D_i(\mathbf{x})$ with space-coordinate dependence. An advantage of using $D_i(\mathbf{x})$ is that one can effectively fix the position of vortex (the zeros of Ψ_i) during the numerical calculation, if one choose $D_i(\mathbf{x})$ appropriately. In order to attain this, we choose a function $D_i(\mathbf{x}) = A\nabla^2\ln\left(|\mathbf{x}-\mathbf{a}_i|^2+\epsilon^2\right) + c$, where $\mathbf{a}_i$ stands for the i-th vortex position and A and c are positive constants. The value of A is taken as an extremely large value to fix the profile of the wave function only near the vortex cores. Also, ϵ should be sufficiently small. We chose $A = 80000$, $\epsilon = 0.01$, and $c = 0.1$ in our numerical computation. We take the Abrikosov ansatz given in Eqs. (30) and (31) as the initial condition at $\tau = 0$ and minimize the energy under the imaginary time evolution. After the solutions converge sufficiently, we calculate the interaction energy Eq. (32).

Throughout our numerical computation below, we will set $m/\hbar^2 = 1$ and $v^2 = 1$. Then we regard m_+ and m_- as independent parameters of the GP equations and perform the numerical calculation by varying them. Remember that $m_+ < m_-$ corresponds to $g_{12} < 0$ (attractive force), whereas $m_+ > m_-$ corresponds to $g_{12} > 0$ (repulsive force). No net interaction exists accidentally when $m_+ = m_-$.

The result is shown in Fig. 3. We compare the intervortex potential obtained numerically and the one obtained analytically. As can be seen, the analytic results reproduce the numerical results quite well. We have only one fitting

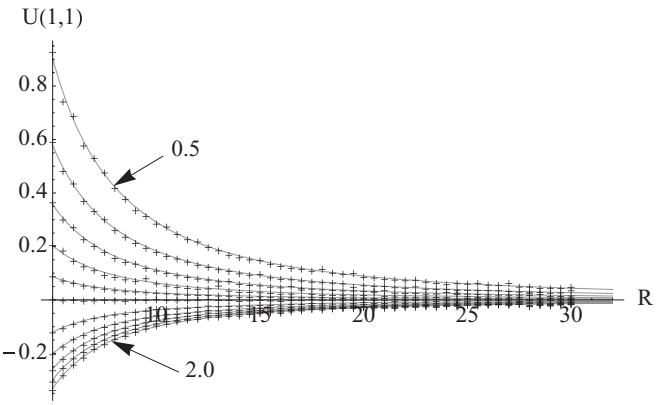

FIG. 3. Plots of the intervortex potential $U_{(1,1)}(R)$ for $m_- = (0.5,0.6,0.7,0.8,0.9,1,1.2,1.4,1.6,1.8,2)$ from top to bottom, with $m_+ = 1$. Solid lines are asymptotic intervortex forces (Abrikosov ansatz), which are analytically obtained in Eq. (35).

parameter 2ξ, which is the the short-range cut-off. The values 2ξ for various choice of m_- for fixed $m_+ = 1$ are shown in Fig. 4. We find the linear dependence of the short-range cut-off ξ on the healing length $1/m_-$.

IV. SUMMARY AND DISCUSSION

We have studied the asymptotic interaction between half-quantized vortices, i.e., (1,0) and (0, ± 1), winding around Ψ_1 and Ψ_2, respectively, in the two-component BEC. Since the two components interact only through the density, the (1,0) vortex does not directly experience the circulation of the (0, ± 1) vortex, so that the result does not depend on the signature of the winding number. The leading order of the force between them is found to be $\sim [\ln(R/\xi) - 1/2]/R^3$, in contrast to the one between the same kind of vortices $\sim 1/R$, which is also well known as the force between vortices in scalar BEC, scalar superfluid, and the XY model and global vortices in relativistic field theories. We have first derived it analytically using the Abrikosov ansatz and the asymptotic profile functions of (1,0) and (0,1) vortices. We have then confirmed it numerically with using the extended imaginary time method for the GP equations. We have found that the short-range cut-off parameter ξ of the vortex interaction linearly depends on the healing length $1/m_-$.

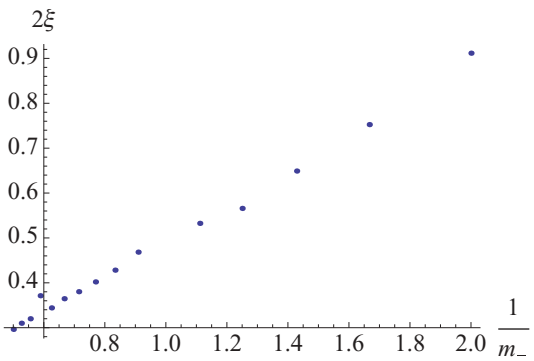

FIG. 4. (Color online) The dependence of the healing length 2ξ on $1/m_-$ with fixed $m_+ = 1$.

The intervortex force will manifest itself in the vortex motion when a pair of (1,0) and (0, ± 1) vortices is prepared in a trapped BEC. Due to the different R-dependence of the intervortex force, the vortex dynamics will be modified from those of the (1,1) or (1, − 1) vortex pairs in the same component, where two vortices orbit around each other for (1,1) and move in parallel for (1, − 1). The details of this dynamic are currently under study. A recent experimental observation of the real-time vortex dynamics [32] will stimulate this kind of study. Our results also suggest a bound state of (1,0) and (0, ± 1) vortices for $g_{12} < 0$. While a set of (1,0) and (0,1) is expected to form a stable integer (mass) vortex (1,1), it is a nontrivial question if (1,0) and (0, − 1) vortices form a bound state, which should be called a (pseudo-) spin vortex. Also, one expects no stable bound states for $g_{12} > 0$. Although there should be instabilities for large separation at least, it does not exclude a possibility of a metastable bound state at short distance. To address these questions, we need to know a short range interaction or stability analysis of the bound states, which remains as a future problem.

Our method should be extended to spinor BECs, which also remains as an interesting future problem. On the other hand, multicomponent systems in relativistic field theories are common in QCD, such as the linear sigma model for the chiral-phase transition and the Landau-Ginzburg model for color superconductors at high baryon density [23]. In these models, order parameters are matrices as in superfluid ^{3}He rather than vectors, and consequently there exist non-Abelian vortices [33]: non-Abelian global vortices in the chiral-phase transition [21] and non-Abelian semi-superfluid vortices in color superconductors at high baryon density [23]. Intervortex forces have been calculated at leading order for non-Abelian global vortices [22] and non-Abelian semi-superfluid vortices [24]; see Ref. [25] for a review. Calculation in the present paper will give the next leading order $[\ln(R/\xi) - 1/2]/R^3$ to them. Especially the force $\cos\alpha/R$ between non-Abelian global vortices at the leading order vanishes for a particular choice ($\alpha = \pm\pi$) of internal orientations of vortices [22], and therefore the next leading order term proportional to

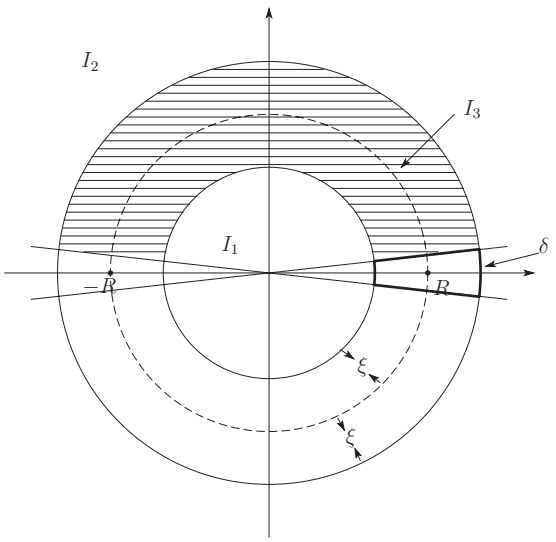

FIG. 5. The integral region to calculate Eq. (A2)

$[\ln(R/\xi) - 1/2]/R^3$ becomes a dominant contribution. An extension of our results to these cases should be important to consider a possibility of vortex lattice phases in heavy-ion collisions or in a neutron star core, as in two-component BEC [2,34–36].

ACKNOWLEDGMENTS

This work was supported by the "Topological Quantum Phenomena" (Grant No. 22103003 and No. 23103515) Grant-in Aid for Scientific Research on Innovative Areas from the Ministry of Education, Culture, Sports, Science and Technology (MEXT) of Japan. The work of M.E. is supported by Special Postdoctoral Researchers Program at RIKEN. The work of K.K. and M.N. is supported in part by Grant-in-Aid for Scientific Research [Grant No. 21740267 (K.K.) and No. 20740141 and No. 23740198 (M.N.)] from the MEXT of Japan.

APPENDIX: DERIVATION OF Eqs. (35) AND (39)

In Eq. (35), we have to evaluate the integral

$$I = \int d^2x \frac{1}{r^2_{(1,0)} r^2_{(0,1)}} = \int d^2x \frac{1}{A_0}, \tag{A1}$$

$$A_0 \equiv r^4 + R^4 - 2r^2R^2\cos 2\theta. \tag{A2}$$

To this end we will use a formula

$$\int_0^{2\pi} d\theta \frac{1}{A + B\cos 2\theta} = \frac{2\pi}{\sqrt{A^2 - B^2}}, \tag{A3}$$

for $A > |B|$. To evaluate Eq. (A2), we divide the integral region as shown in Fig. 5. In addition to I_1 and I_2, we take into account the contributions I_3 from the strip of width 2ξ. Since the integrand diverges at $(x,y) = (\pm R, 0)$, we introduce an ultraviolet cut-off ξ. Then, we will remove the small region that includes the points of vortex positions. Hence, the total integral is written as

$$I_{\text{cut-off}} = I_1 + I_2 + 2I_3. \tag{A4}$$

For $R \gg \xi$, the integrals I_1 and I_2 are calculated as

$$I_1 = \int_0^{R-\xi} \frac{2\pi r dr}{R^4 - r^4} \simeq \frac{\pi}{2R^2}\left[\ln\frac{R}{\xi} + O\left(\frac{\xi}{R}\right)\right], \tag{A5}$$

$$I_2 = \int_{R+\xi}^{\infty} \frac{2\pi r dr}{R^4 - r^4} \simeq \frac{\pi}{2R^2}\left[\ln\frac{R}{\xi} + O\left(\frac{\xi}{R}\right)\right], \tag{A6}$$

where we have used Eq. (A3). The remaining integral

$$I_3 = \int_{R-\xi}^{R+\xi} dr \int_{\delta}^{\pi-\delta} d\theta \frac{r}{A_0}, \tag{A7}$$

with $\xi/R \ll 1$ and $\delta \ll 1$ is evaluated as follows. Note that $\cos 2\theta \leqslant \cos 2\delta = 1 - 2\delta^2 + \cdots < 1 - \delta^2$ and $A_0 > (r^2 - R^2)^2 + 2r^2R^2\delta^2 \geqslant 2r^2R^2\delta^2$. Thus, we have the following inequality

$$0 \leqslant I_3 \leqslant \frac{\pi - 2\delta}{2R^2\delta^2} \ln\frac{R+\xi}{R-\xi} \simeq \frac{\pi}{R^2\delta^2}\frac{\xi}{R}. \tag{A8}$$

Thus, for any δ, one can choose sufficiently small ξ, so that I_3 becomes negligibly small.

In summary, we get

$$I_{\text{cut-off}} = \frac{\pi}{R^2}\left[\ln\frac{R}{\xi} + O\left(\frac{\xi}{R}\right)\right]. \tag{A9}$$

Next, we calculate the integration in Eq. (39),

$$J = \int d^2x\, \vec{\nabla}\theta_{(1,0)} \cdot \vec{\nabla}\theta_{(0,1)} = \int d^2x \frac{r^2 - R^2}{r^2_{(1,0)} r^2_{(0,1)}}$$

$$= \int dr d\theta \frac{r(r^2 - R^2)}{r^4 + R^4 - 2r^2R^2\cos 2\theta}. \tag{A10}$$

By using Eq. (A3), one can first perform the integration in θ and then integrate with respect to r as

$$J = \int_0^{\infty} dr \frac{2\pi r(r^2 - R^2)}{\sqrt{(r^4 - R^4)^2}}$$

$$= \lim_{L\to\infty}\left[-\int_0^R \frac{2\pi r dr}{r^2 + R^2} + \int_R^L \frac{2\pi r dr}{r^2 + R^2}\right]$$

$$= \lim_{L\to\infty} \pi \ln\frac{L^2 + R^2}{4R^2}. \tag{A11}$$

[1] T. L. Ho and V. B. Shenoy, Phys. Rev. Lett. **77**, 3276 (1996); E. Timmermans, *ibid.* **81**, 5718 (1998); B. V. Schaeybroeck, Phys. Rev. A **78**, 023624 (2008).

[2] K. Kasamatsu, M.Tsubota, and M. Ueda, Int. J. Mod. Phys. B **19**, 1835 (2005).

[3] G. W. Semenoff and F. Zhou, Phys. Rev. Lett. **98**, 100401 (2007); M. Kobayashi, Y. Kawaguchi, M. Nitta, and M. Ueda, *ibid.* **103**, 115301 (2009).

[4] H. T. C. Stoof, E. Vliegen, and U. Al Khawaja, Phys. Rev. Lett. **87**, 120407 (2001); J.-P. Martikainen, A. Collin, and K.-A. Suominen, *ibid.* **88**, 090404 (2002); C. M. Savage and J. Ruostekoski, Phys. Rev. A **68**, 043604 (2003).

[5] T. L. Ho, Phys. Rev. Lett. **81**, 742 (1998); U. Leonhardt and G. E. Volovik, JETP Lett. **72**, 46 (2000); A. E. Leanhardt, Y. Shin, D. Kielpinski, D. E. Pritchard, and W. Ketterle, Phys. Rev. Lett. **90**, 140403 (2003).

[6] J. Ruostekoski and J. R. Anglin, Phys. Rev. Lett. **86**, 3934 (2001); R. A. Battye, N. R. Cooper, and P. M. Sutcliffe, *ibid.* **88**, 080401 (2002); C. M. Savage and J. Ruostekoski, *ibid.* **91**, 010403 (2003).

[7] U. A. Khawaja and H. T. C. Stoof, Nature (London) **411**, 918 (2001); Phys. Rev. A **64**, 043612 (2001).

[8] M. A. Metlitski and A. R. Zhitnitsky, J. High Energy Phys. 06 (2004) 017; J. Ruostekoski, Phys. Rev. A **70**, 041601(R) (2004);

[9] Y. Kawaguchi, M. Nitta, and M. Ueda, Phys. Rev. Lett. **100**, 180403 (2008).

[10] K. Kasamatsu, H. Takeuchi, M. Nitta, and M. Tsubota, J. High Energy Phys. 11 (2010) 068.

[11] M. Ueda and Y. Kawaguchi, e-print arXiv:1001.2072 (2010).

[12] Y. Kawaguchi, M. Kobayashi, M. Nitta, and M. Ueda, Prog. Theor. Phys. Suppl. **186**, 455 (2010).

[13] A. Achucarro and T. Vachaspati, Phys. Rep. **327**, 347 (2000)

[14] M. B. Hindmarsh and T. W. B. Kibble, Rep. Prog. Phys. **58**, 477 (1995).
[15] A. Vilenkin and E. P. S. Shellard, *Cosmic Strings and Other Topological Defects* (Cambridge Univ. Press, New York, 1994).
[16] C. J. Pethick and H. Smith, *Bose-Einstein Condensation in Dilute Gases*, 2nd ed. (Cambridge University Press, New York, 2008).
[17] A. Vilenkin and A. E. Everett, Phys. Rev. Lett. **48**, 1867 (1982).
[18] E. P. S. Shellard, Nucl. Phys. B **283**, 624 (1987).
[19] L. Perivolaropoulos, Nucl. Phys. B **375**, 665 (1992).
[20] R. L. Davis and E. P. S. Shellard, Phys. Rev. Lett. **63**, 2021 (1989); R. L. Davis, Phys. Rev. D **40**, 4033 (1989); B. A. Gradwohl, G. Kaelbermann, T. Piran, and E. Bertschinger, Nucl. Phys. B **338**, 371 (1990).
[21] A. P. Balachandran and S. Digal, Phys. Rev. D **66**, 034018 (2002); M. Nitta and N. Shiiki, Phys. Lett. B **658**, 143 (2008); M. Eto, E. Nakano, and M. Nitta, Nucl. Phys. B **821**, 129 (2009).
[22] E. Nakano, M. Nitta, and T. Matsuura, Phys. Lett. B **672**, 61 (2009).
[23] A. P. Balachandran, S. Digal, and T. Matsuura, Phys. Rev. D **73**, 074009 (2006); M. Eto and M. Nitta, *ibid.* **80**, 125007 (2009); M. Eto, E. Nakano, and M. Nitta, *ibid.* **80**, 125011 (2009); M. Eto, M. Nitta, and N. Yamamoto, Phys. Rev. Lett. **104**, 161601 (2010); Phys. Rev. D **83**, 085005 (2011); Y. Hirono, T. Kanazawa, and M. Nitta, *ibid.* **83**, 085018 (2011); S. Yasui, K. Itakura, and M. Nitta, *ibid.* **81**, 105003 (2010); Phys. Rev. B **83**, 134518 (2011)
[24] E. Nakano, M. Nitta, and T. Matsuura, Phys. Rev. D **78**, 045002 (2008).
[25] E. Nakano, M. Nitta, and T. Matsuura, Prog. Theor. Phys. Suppl. **174**, 254 (2008).
[26] G. Thalhammer, G. Barontini, L. De Sarlo, J. Catani, F. Minardi, and M. Inguscio, Phys. Rev. Lett. **100**, 210402 (2008).
[27] S. B. Papp, J. M. Pino, and C. E. Wieman, Phys. Rev. Lett. **101**, 040402 (2008).
[28] S. Tojo, Y. Taguchi, Y. Masuyama, T. Hayashi, H. Saito, and T. Hirano, Phys. Rev. A **82**, 033609 (2010).
[29] M. R. Matthews, B. P. Anderson, P. C. Haljan, D. S. Hall, C. E. Wieman, and E. A. Cornell, Phys. Rev. Lett. **83**, 2498 (1999).
[30] P. Öhberg and L. Santos, Phys. Rev. A **66**, 013616 (2002).
[31] This behavior is the same for global non-Abelian vortices appearing in the chiral-phase transition of QCD; see the second reference in [[21]]. Similar holds for semi-superfluid non-Abelian vortices in color superconductors of QCD at high density; see the second reference in [23].
[32] D. V. Freilich, D. M. Bianchi, A. M. Kaufman, T. K. Langin, and D. S. Hall, Science **329**, 1182 (2010).
[33] The terminology "non-Abelian vortices" here denotes vortices in symmetry breaking of G to H with a non-Abelian group H and $\pi_1(G/H) \neq 0$.
[34] V. Schweikhard, I. Coddington, P. Engels, S. Tung, and E. A. Cornell, Phys. Rev. Lett. **93**, 210403 (2004).
[35] E. J. Mueller and T. L. Ho, Phys. Rev. Lett. **88**, 180403 (2002).
[36] K. Kasamatsu, M. Tsubota, and M. Ueda, Phys. Rev. Lett. **91**, 150406 (2003).